

Multiple scattering in evolving media

Roel Snieder and John Page

With high sensitivity to evolving environments, multiply scattered acoustic and elastic waves are being used to probe temporal changes in physical systems, from volcanoes to bubbles in a turbulent fluid.

Roel Snieder is the W. M. Keck Distinguished Professor of Basic Exploration Science in the Center for Wave Phenomena and the department of geophysics at the Colorado School of Mines in Golden, Colorado. **John Page** is a professor of physics and director of the ultrasonics research laboratory in the department of physics and astronomy at the University of Manitoba in Winnipeg, Canada.

Singly scattered waves form the basis of many imaging techniques that are used, for example, in radar and in seismic exploration. If one knows the arrival time of a singly scattered wave, along with its velocity and direction of propagation, one can determine the location of the scatterer. For multiply scattered waves it is more difficult to determine the locations of the scatterers because the waves propagate over many possible scattering trajectories involving a number of scatterers. Thus, multiply scattered waves are not so useful for imaging.

Multiply scattered waves are very useful, however, for detecting temporal changes in the medium through which they propagate. The changes may arise from the motion of the scatterers, changes in their scattering properties, or changes in the properties of the matrix in which the scatterers are embedded. The singly scattered wave in figure 1a traverses the medium at most twice. By contrast, the multiply scattered waves in figure 1b travel along much longer trajectories through the medium. Because of their much greater spatial sampling, multiply scattered waves are much more sensitive to changes in the medium than are singly scattered

waves. This applies both to waves that are truly multiply scattered within the medium and to reverberant waves that bounce back and forth between the medium's boundaries (figure 1c). We refer to both types of waves as multiply scattered waves, despite the difference in the mechanism that causes them to repeatedly sample the changes in the medium.

An example of multiply scattered waves is given in figure 2, which shows the ground motion recorded on Mount Merapi, an active volcano in Indonesia. The waves, excited by an air gun placed on the side of the volcano and recorded on a nearby seismograph, do not consist of isolated discrete arrivals but rather of a wavetrain of interfering scattered waves. Seismologists refer to these scattered waves as coda waves, after the Latin word for "tail." Volcanoes strongly scatter elastic waves, and the coda waves recorded on Mount Merapi are dominated by multiple scattering: The distance between scattering events, as measured by the scattering mean free path (about 400 m), is much smaller than the path length covered by the waves in figure 2 (up to about 50 km, or 125 scattering events).¹

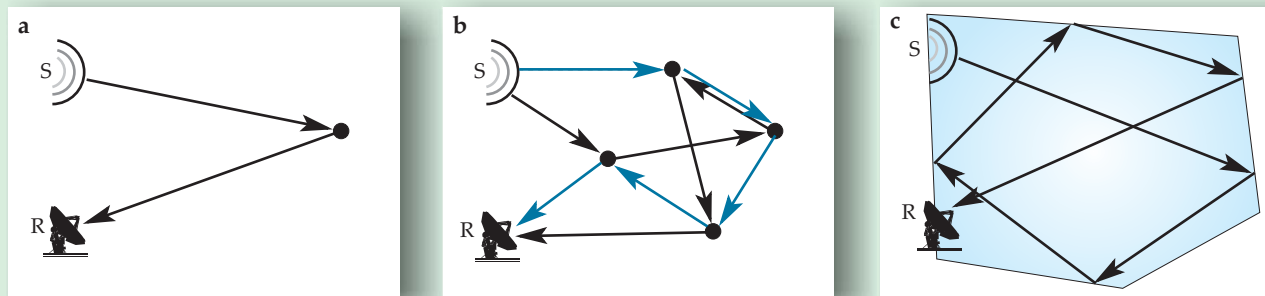


Figure 1. Singly versus multiply scattered waves. Singly scattered waves (a) that propagate from a source S to a receiver R traverse a region of space at most twice, while multiply scattered waves (b) can propagate many times in the same region. Reverberant waves (c) that bounce between boundaries can also sample the same region repeatedly.

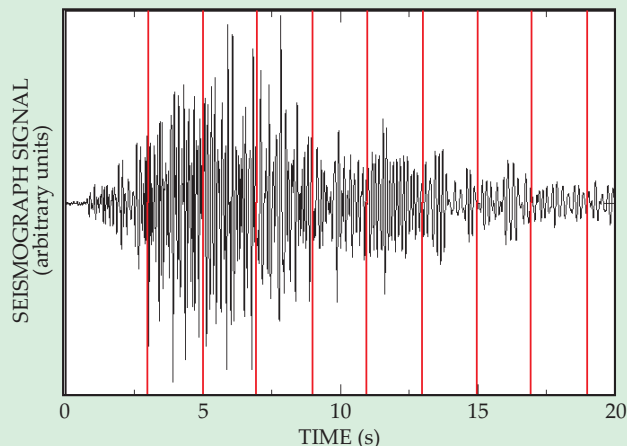


Figure 2. The vertical component of the ground motion recorded on 30 June 1998 on Mount Merapi, an Indonesian volcano. The waves are excited by an air gun on the side of the volcano a few kilometers away. The vertical red lines break the time series into independent windows for cross-correlating the data. (Data courtesy of Ulrich Wegler.)

An interferometer extracts small changes in parameters by using the sensitivity of waves that are repeatedly reflected. A strongly scattering medium acts as a natural interferometer because the waves scattered along different multiple-scattering paths interfere, which produces a complicated spatial pattern of nodes and antinodes. This interference pattern, known as speckle, is highly sensitive to changes in the medium because of the long path lengths involved. The coda waves can be seen as a speckle pattern in time and are also highly sensitive to changes in the medium. If the multiply scattered waves are excited before, after, or repeatedly during a temporal change in the medium, then one can exploit the sensitivity of the waves to quantify the change. In acoustics this technique is referred to as diffusing acoustic wave spectroscopy² (by analogy with diffusing wave spectroscopy in optics³) and in seismology as coda wave interferometry.⁴

Monitoring problems contain two different time scales.

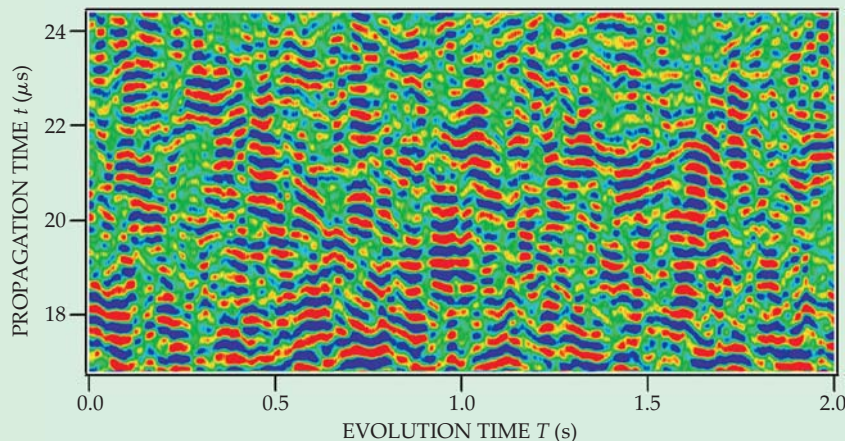
The propagation time t denotes the time of flight of the scattered waves relative to the moment of excitation (as in figure 2). The evolution time T marks the time at which a wave is excited, and as its name implies, it also denotes the time period over which the medium has changed. Figure 3, which shows acoustic waves that have been scattered by a suspension of bubbles in water, illustrates the two time scales. The motion of the bubbles as the evolution time increases constitutes a change in the medium through which the sound waves propagate, and variations in the recordings of scattered waves encode that motion. The changes are more pronounced for long propagation times (top of figure) because waves that arrive later have been scattered more often and are therefore more sensitive to changes in the location of scatterers. Figure 4 illustrates this increased sensitivity more directly with snapshots of the scattered wavetrains at different evolution times for two quite different media: a fluid suspension of particles and Mount Merapi. In both cases the initially arriving waves show almost no change with evolution time, whereas large changes are seen at later propagation times.

The evolution time in figure 3 is five orders of magnitude longer than the propagation time. If the evolution time were comparable to the propagation time, the description of the wave propagation would be more complicated because one would need to account for wave scattering by moving scatterers. Also, one would need to consider the evolution of the medium during the propagation of the pulse. In this article we focus on the many applications for which T is much greater than t . In that limit the scatterers can be considered to be static during the wave propagation, and the sensitivity of multiply scattered waves to small changes in the medium is especially useful.

Probing suspension dynamics

We illustrate these principles by first showing how multiply scattered acoustic waves can be used as a sensitive probe of the motion of particles—or bubbles—that are suspended in a fluid. Since only longitudinally polarized acoustic waves can propagate through the suspension, the scattering is simpler than for the elastic waves discussed below. However, understanding the dynamics of a suspension is surprisingly challenging, due to the particles' long-range interactions, which are mediated by the intervening fluid. These hydrodynamic interactions lead to correlations in the motion of the particles at short length scales and to large, apparently random motion at longer length scales. The behavior can be characterized by

Figure 3. Pressure fluctuations of scattered acoustic waves as a function of wave propagation time t and evolution time T , the time at which the waves were sent through a suspension of bubbles in water. Positive fluctuations are in red, negative fluctuations in blue. At long propagation times, the waves are more sensitive to bubble motion that has occurred during the evolution time. (Data courtesy of Anatoliy Strybulevych and Tomohisa Norisuye.)



the particle velocity correlation function, whose correlation length ξ measures the range over which the particles move together. Because the complex motions are difficult to model accurately, new methods to probe the spatial correlations and fluctuations are potentially important for understanding the physics of fluidized or sedimenting suspensions, as well as related problems in the physics of mixing.

As a model system, consider a suspension of 1-mm-diameter glass spheres in a liquid consisting of a mixture of water and glycerol. When the wavelength of incident ultrasound is comparable to the particle size, the system exhibits strong multiple scattering for a wide range of particle volume fractions ϕ ; for the example shown in figure 4a, $\phi = 0.40$ and the mean free scattering time is $0.5 \mu\text{s}$, so that the waves at the longest propagation times shown have been scattered many times. As the particles move, the changes in the scattered wave field, shown in the right side of figure 4a, exhibit no net time shift to earlier or later times but are instead characterized by fluctuations in both amplitude and phase. These temporal field fluctuations can be quantitatively related to the motion of the particles by looking at the autocorrelation function of the scattered wave field at a given propagation time t (see the box on page 53). Selecting a long propagation time maximizes sensitivity to small particle displacements; a short propagation time allows the evolving dynamics to be watched for long time intervals.

If all scatterers were to move together uniformly, the speckle pattern would simply move too (at least for a planar incident pulse), since the paths between scatterers would remain fixed. In the more interesting case of nonuniform motion, the change in the scattered waves is governed by the relative motion of the scatterers. As discussed in the box, the field autocorrelation function is directly related to the relative mean square displacement $\langle \Delta r_{\text{rel}}^2(\Delta T, l^*) \rangle$, during the evolution time interval ΔT , of particles separated by the transport mean free path l^* , the average step length of the sound's random-walk paths through the sample.² Measuring the relative motion of particles separated by a known average distance gives valuable information about the fluctuations and correlations of the particle displacements as a function of time.

Figure 5 presents representative data and analysis. There, $\langle \Delta r_{\text{rel}}^2(\Delta T, l^*) \rangle$ is found to increase quadratically with evolution time. Thus, at least for short evolution times, the particles move with constant velocities along ballistic trajectories with a root mean square relative velocity $\Delta V_{\text{rel}}(l^*) = \sqrt{\langle \Delta r_{\text{rel}}^2(\Delta T, l^*) \rangle / (\Delta T)^2}$ that can be determined directly. By varying the ultrasound frequency, one can vary the strength of the scattering and hence l^* , so the relative velocity of particles in the suspension can be measured over a wide range of distances between particles. At short distances the relative velocity increases with distance, but at large distances it levels off to $\sqrt{2}V_{\text{rms}}$, where V_{rms} is the absolute rms particle velocity (see figure 5b). From such data, the particle velocity correlation function can be determined. Measurements of the correlation function show an exponential decay with distance, and the decay rate gives the correlation length ξ . For separations below ξ , the particles move more or less in unison.²

Such measurements are important for helping to understand the mechanisms that determine the magnitude of the correlation length, which plays a key role in governing the dynamics. Thus, multiply scattered ultrasonic waves can provide quantitative information on the dynamics of suspensions, information that is relevant both to fundamental studies of the motion in suspensions and turbulent fluids and to

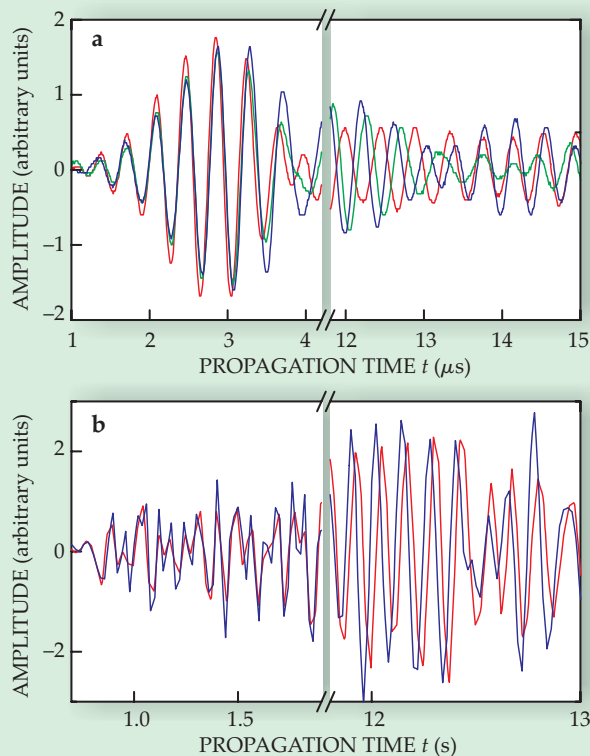


Figure 4. Signatures of change. (a) Segments of multiply scattered ultrasonic waves transmitted through a particulate suspension, monitored at three evolution times 60 ns apart. The waveforms are similar for short propagation times, but they show strong variations in amplitude and phase at later propagation times. (b) Waveforms excited by an air gun on Mount Merapi on 30 June (red) and 14 July 1998 (blue) and recorded on a seismograph about 2 km away. A change in the sound speed can be inferred from the distinct phase shift. (Data courtesy of Michael Cowan and Ulrich Wegler.)

practical applications such as monitoring mixing processes, fluidized beds, and slurry flow.

Monitoring Mount Merapi

Multiply scattered waves are also used in seismology, on time and length scales very different from those of acoustic waves in suspensions. To illustrate the technique, we consider data acquired on Mount Merapi.⁵ In contrast to acoustic waves scattered by particles in suspension, the multiply scattered waves recorded on Mount Merapi show a distinct phase shift but little change in the wave shape (see figure 4b). Such data indicate a change in seismic velocity.

These changes in the waveforms can be extracted using the time-shifted cross-correlation of the waveforms at different evolution times (see the box). In the Merapi data, the dominant change in the waveforms is a change in the arrival time of the coda waves. That change can be extracted from the time-shifted cross-correlation for several nonoverlapping time windows, such as the time intervals indicated in figure 2. For a spatially homogeneous velocity change $\Delta c/c$, the travel-time change $\langle \tau \rangle$ for a time interval centered at time t is given by $\langle \tau \rangle / t = \Delta c/c$.⁴ Splitting the data into several nonoverlapping time windows makes it possible to quantify the uncertainty in the inferred change of the seismic velocity, but

only if the source of the waves is a short pulse; for other sources, such as monochromatic waves, the information from nonoverlapping time windows is not independent. For the data in figure 4b, the velocity change is 0.25%.

The velocity change in elastic media depends on that of longitudinal waves, shear waves, and surface waves.⁶ Ulrich Wegler and Christoph Sens-Schönfelder have monitored the velocity change at Mount Merapi. Looking at the seasonal variation in the velocity change, they found a correlation between seismic velocity and precipitation.⁷ Changes in precipitation affect the water table, which in turn changes the shear modulus near the surface. A change in shear modulus modifies the velocity of shear waves, and to a lesser extent the velocity of compressional waves. Since the change in the water table is confined to the near-surface, it is likely that the coda waves recorded on Mount Merapi are dominated by surface waves.

Other applications

The examples above illustrate two of the main types of changes that have been studied using multiply scattered waves—motion of scatterers and changes in wave velocity. These different perturbations leave a different imprint on the changes in the scattered waveforms, and their analyses can be generalized to obtain useful information about a much wider range of situations. Georges Poupinet has pioneered applications in the geosciences, and multiply scattered elastic waves are now being used to detect changes in volcanoes and fault zones and have been used to monitor changes in stress in the subsurface.⁸ Changes in the seismic velocity can be due to variations in temperature, fluid content, and possibly fracture formation.^{4,9} Monitoring these quantities is important for detecting environmental problems, managing aquifers and hydrocarbon reservoirs, and monitoring natural hazards such as volcanoes, fault zones, and landslides.¹⁰ The technique can potentially be used in nondestructive testing for fracture or crack formation. A change in source location, as well, can be inferred from coda wave interferometry,¹¹ which can be used for high-precision location of earthquakes and microseismic events under field conditions with an accuracy that cannot be attained using directly transmitted waves.

Multiply scattered elastic waves are also being used in ultrasound experiments⁹ to study changes in solids due to temperature changes and fluid infiltration. The results shed light on the dependence of elastic moduli on temperature and fluid content, and hence on the mechanics of solids. Of particular interest is the work of Oleg Lobkis and Richard Weaver, who used changes in the wave shape with temperature in an aluminum sample to estimate the rate of energy transfer between compressional waves and shear waves at the free surface and thus obtain information on the rate at which equipartition of energy between the waves was reached. At intermediate frequencies between ultrasonic and seismic, coda wave interferometry is being used to monitor

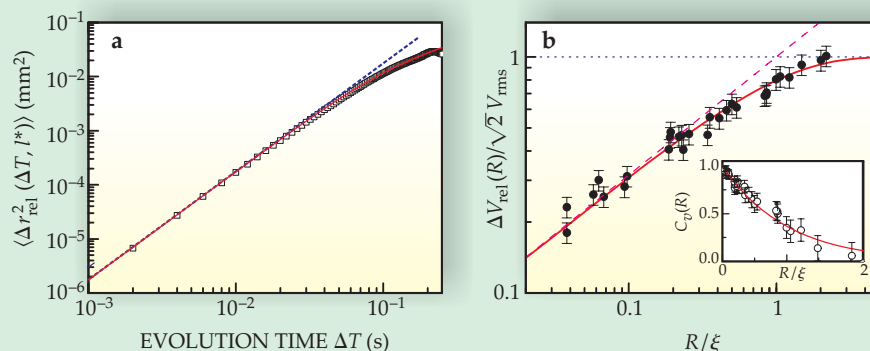


Figure 5. Determining suspension properties. (a) The relative mean square displacement, as a function of time interval ΔT , of beads in suspension. The data, extracted from the autocorrelation function calculated from the measured wave fluctuations in scattered ultrasound, scale as $(\Delta T)^2$ (dashed line) for short times, and also depend on the transport mean free path, l^* . (b) The dependence of the relative particle velocity ΔV_{rel} on the distance R between particles. The relative velocity has been scaled by the particles' root mean square velocity, and the distance has been scaled by the particle correlation length ξ . The inset shows the particle velocity correlation function deduced from the measurements. (Adapted from ref. 2.)

concrete structures nondestructively;¹² the success of initial measurements by Eric Larose and coworkers, who measured the changes in the wave velocity of the concrete due to temperature, suggests that other applications, such as detecting changes due to stress loading, damage, aging, or crack formation, are feasible too. Thus, there is considerable promise in using multiply scattered elastic waves to monitor the structural integrity of buildings and other infrastructure.

Diffusing acoustic wave spectroscopy provides a novel and useful method for investigating the complex dynamical behavior of suspensions and is providing insights into how the dynamics are influenced by the concentration of particles or bubbles, the size of the system in which they are contained, and the Reynolds number, which measures the relative importance of viscous and inertial effects in the hydrodynamic interactions between the scatterers. In addition, since both phase and amplitude information can be measured directly,^{2,13} the technique is being used to investigate mesoscopic wave physics in the multiple-scattering regime, where the role of phase is important but not often observed directly. For dynamic media such as particulate or bubbly suspensions, progress in developing appropriate statistical measures of phase fluctuations is revealing a fundamental relationship between the variance of the phase along a particular scattering path, which is measured by the field autocorrelation function, and the phase measured in experiments, which results from the superposition of the wave field from all scattering paths.¹³ Such a connection allows direct measurements of phase fluctuations to be used in monitoring the dynamics. That approach may be advantageous when amplitude noise is a problem, since such noise degrades measurements of the field correlation function more than it affects phase measurements.

Practical applications of diffusing acoustic wave spectroscopy include process control and monitoring of the flow of slurries in pipelines and performance optimization of chemical reactors in which solid catalyst particles, gases, and liquid reactants must all be brought into contact. For these slurry bed reactors, the capability for online monitoring of instabilities that degrade performance may be especially valuable.

Quantifying changes

As the evolution time T of the medium increases, the changes in the scattered wave field $\psi(t, T)$ can be related to changes in the medium by investigating the autocorrelation of the field at a fixed propagation time t . The autocorrelation function g_1^{AC} quantifies the extent to which the field at propagation time t varies after an evolution time interval ΔT :

$$g_1^{AC}(t, \Delta T) = \frac{\int \psi(t, T) \psi^*(t, T + \Delta T) dT}{\int |\psi(t, T)|^2 dT} \simeq \langle e^{-i\Delta\phi_p(\Delta T)} \rangle, \quad (1)$$

where $\Delta\phi_p$ is the change in phase along path p during the time interval ΔT , and $\langle \cdot \rangle$ indicates an ensemble average over all paths that reach the detector at propagation time t . The path phase change is characterized by its average $\langle \Delta\phi_p \rangle$ and its variance σ_ϕ^2 , which measures the fluctuations. In terms of these variables, the real part of g_1 is

$$g_1^{AC}(\Delta T) \simeq \cos(\langle \Delta\phi_p \rangle) \exp(-\sigma_\phi^2/2). \quad (2)$$

The exponential factor reflects the fact that for $\Delta\phi_p$ the deviations from the average follow a Gaussian distribution because of the central limit theorem.

For the case of moving scatterers (see figures 4a and 5), the average phase change $\langle \Delta\phi_p \rangle$ is zero, but the variance σ_ϕ^2 is not—it reflects the fluctuations in the relative displacement of the scatterers for each step along the multiple scattering paths. The field autocorrelation function may then be written as follows:²

$$g_1^{AC}(\Delta T) \approx \exp\left[-\frac{Nk^2}{6} \langle \Delta r_{rel}^2(\Delta T, l^*) \rangle\right]. \quad (3)$$

Here, N is the average number of times the waves scatter in time t , and k is the wave vector. Equation 3 shows how g_1^{AC} can be used to measure the relative mean square displacement $\langle \Delta r_{rel}^2 \rangle$ of the scatterers as a function of evolution time and distance between the scatterers, the latter characterized by the average step length l^* of the multiply scattered waves. This approach is especially straightforward when the average phase shift is zero.

Diffusing acoustic wave spectroscopy works best for concentrated suspensions, in which multiple scattering is strong. But it is also possible to study weakly scattering systems if they are contained in a reverberant cavity so that the ultrasonic waves diffuse not by volume scattering but by multiple reflections off the walls of the cavity (see figure 1c). This reverberant technique, called diffusing reverberant acoustic wave spectroscopy, can be used not only to study scatterer motion but also to obtain the scattering mean free path, l_s , which measures the attenuation of waves due to scattering.¹⁴ The simplest way to determine l_s from reverberant waves is to compare the propagation-time dependence of the average field (in which the effects of scattering cancel) to the average intensity (in which they do not): $\langle \psi(t) \rangle^2 / \langle \psi(t)^2 \rangle \approx e^{-ct/l_s}$. The technique can be used to measure the scattering cross section σ if the number density of scatterers n is known, or vice versa, since $l_s = 1/n\sigma$. This technique is being used by Julien de Rosny, Philippe Roux, Stéphane Conti, and David Demer for counting and sizing fish in aquaculture and, by exploiting the correlations of the reverberant fields, for moni-

toring fish motion as well. They have also used the technique to measure the acoustic properties and dynamics of people moving on a squash court, which has given new information on the sound scattering and absorption properties of the human body.¹⁴ Such information is of interest for understanding and modeling the effects of humans on the acoustics of concert halls and other public buildings.

Multiply scattered ultrasonic waves are also starting to be used to characterize the dynamic properties of heterogeneous food materials. Although many foods absorb ultrasound too strongly for multiply scattered waves to be detected, there are important exceptions, such as bubbly drinks and aerated food gels. The elegance of bubble dynamics in a carbonated beverage is a critical aspect of the beverage's appearance—a prime quality attribute (along with appealing “mouthfeel”) that manufacturers seek to optimize. The underlying physics of bubble formation, growth, and upward motion in complex fluids such as champagne¹⁵ and beer is also of continuing interest (see the article by Neil Shafer and Richard Zare in PHYSICS TODAY, October 1991, page 48). Thus,

$$g_1^{CC}(T, \Delta t) = \frac{\int_{t-w}^{t+w} \psi(t', 0) \psi(t' + \Delta t, T) dt'}{\left[\int_{t-w}^{t+w} \psi^2(t', 0) dt' \int_{t-w}^{t+w} \psi^2(t', T) dt' \right]^{1/2}}, \quad (4)$$

where Δt denotes the time shift used in the cross-correlation. This cross-correlation has a maximum for a time shift Δt_{max} that optimally matches the two waves. The time Δt_{max} gives the average of the travel time changes $\tau_p = \Delta\phi_p/\omega$ of each multiple-scattering path p that arrives in the time window,⁴ weighted by the path intensity I_p :

$$\Delta t_{max} = \langle \tau_p \rangle = \frac{\sum_p \tau_p I_p}{\sum_p I_p}. \quad (5)$$

Changes in wave velocity can be directly measured from $\Delta t_{max} = \langle \tau_p \rangle = \langle \Delta\phi \rangle / \omega$.

The maximum value $g_{1,max}^{CC}$ of the cross-correlation becomes less than 1 as the waveforms change. For small decorrelations, this maximum is given by

$$g_{1,max}^{CC} = 1 - \frac{1}{2} \overline{\omega^2 \sigma_\tau^2}, \quad (6)$$

with $\overline{\omega^2}$ the mean squared angular frequency, and $\sigma_\tau^2 = \sigma_\phi^2 / \overline{\omega^2}$ the variance of the intensity-weighted travel time perturbation.⁴ Equation 6 can be recognized as a Taylor expansion of the exponential factor in equation 2.



Figure 6. Monitoring bubbles in beer. A one-microsecond-long ultrasound pulse, at a center frequency of 1 MHz, is generated near the top of a mug of beer using an immersion transducer (top left) and detected with a needle-shaped hydrophone (top center). After many reflections off the mug's walls, the detected waves are sensitive to the evolution of the bubbles even when the bubble concentration is very low. (Photo courtesy of Valentin Leroy.)

using multiply scattered ultrasonic waves to monitor bubble evolution (bubble sizes, growth rates, formation frequency, velocities, and concentrations) is potentially valuable, especially since the technique can be used in optically opaque materials. For example, bubbles in beer can be monitored using either multiply scattered or reverberant ultrasonic waves, depending on the bubble concentration and frequency (figure 6). Quantitative interpretation of such data in a range of aerated food materials will allow new non-destructive methods, possibly including online process control applications, to be developed for monitoring food quality and texture.

In the absence of control

The examples shown here involve a controlled, repeatable source, but such a source isn't always available. Repeat earthquakes can sometimes be used in geoscience applications for monitoring, but due to the irregular spatial and temporal occurrence of repeatable earthquakes, this is not always feasible. A recent development is the extraction of the impulse response

for wave propagation—that is, the Green function—using ambient fluctuations, as pioneered in ultrasonics by Weaver and Lobkis and in seismology by Anne Paul and Michel Campillo.¹⁶ By cross-correlating broadband noisy signals at two or more detectors, one can extract the coherent part of the signal that propagates between the detectors; that approach gives the same information that would be obtained by actively generating and detecting waves at those locations using impulsive sources. By either transmission tomography or imaging techniques based on reflected or scattered waves, the extracted waves can be used to create images of heterogeneities in the medium through which the waves propagate. Alternatively, repeated extraction of the impulse response can be used for monitoring changes in the medium.

The extraction of impulse responses is illustrated in figure 7. Accelerometers in the basement and 10 floors of the Millikan Library at Caltech recorded the building's motion during the 2002 Yorba Linda earthquake. Since the motion was excited by incoherent waves, it cannot easily be used to measure the mechanical properties of the building—the motion depends on the unknown excitation and on the building response. Also, different earthquakes will excite the building in different ways, which makes it impossible to use a direct comparison of waveforms to detect changes in the structural integrity of the building. Such a comparison is possible, however, when the building's impulse response can be extracted from the incoherent motion by cross-correlation or deconvolution.

Figure 7b shows the impulse response found from two independent recordings of incoherent motion in the building.¹⁷ The responses correspond to the motion of the building when it is excited impulsively at its base. The two ex-

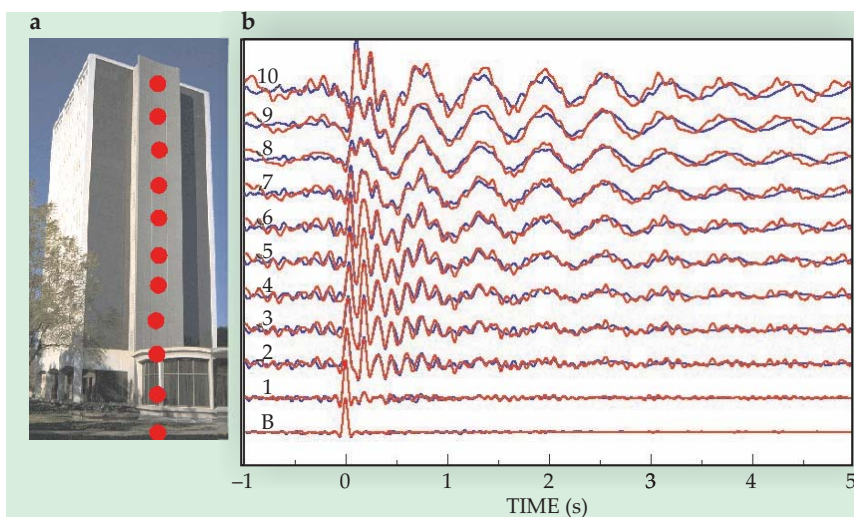


Figure 7. Monitoring building changes. (a) Accelerometers (indicated by red circles) in the Millikan Library at Caltech recorded the motion on various floors during the 2002 Yorba Linda earthquake. (b) The waveforms from two independent recordings, after deconvolution with the bottom floor's motion. (The numbers indicate the building floor.) The waveforms represent each floor's response to an incident impulse at the bottom floor. (Adapted from ref. 17.)

traced wave fields are very similar, which confirms the validity of the technique. From the damped oscillations in the responses, one can estimate the attenuation or quality factor of the building. The motion of a building during sustained shaking depends on the balance between the excitation by the ground motion and the dissipation in the building. The attenuation therefore is a crucial design parameter for structural integrity.

The impulse response can be obtained from recorded incoherent waves, and one can monitor changes in the response on a quasi-continuous basis without the need for a controlled source. This ambient-noise approach has recently been used to monitor Mount Merapi and a fault zone on a daily basis⁷ and to create with unprecedented detail a map of seismic wave velocity in southern California.¹⁸

Monitoring methods based on multiply scattered waves combine modest hardware requirements with a high sensitivity for detecting changes. For acoustic and elastic waves, the sensitivity, as well as the range of phenomena that can be studied, is enhanced by the ability to directly detect changes in both amplitude and phase. Already, the approach has led to a surprisingly diverse number of applications. There is much potential for future development of new applications in physics, the geosciences, and engineering across a wide range of space and time scales.

References

1. U. Wegler, *J. Geophys. Res.* **109**, B07303 (2004).
2. M. L. Cowan, J. H. Page, D. A. Weitz, *Phys. Rev. Lett.* **85**, 453 (2000); M. L. Cowan et al., *Phys. Rev. E* **65**, 066605 (2002); J. H. Page et al., in *Wave Scattering in Complex Media: From Theory to Applications*, B. A. van Tiggelen, S. Skipetrov, eds., Kluwer, Boston (2003), p. 151.

3. D. A. Weitz, D. J. Pine, in *Dynamic Light Scattering: The Method and Some Applications*, W. Brown, ed., Oxford U. Press, New York (1993), p. 652.
4. R. Snieder et al., *Science* **295**, 2253 (2002); R. Snieder, *Pure Appl. Geophys.* **163**, 455 (2006).
5. U. Wegler, B. G. Lühr, A. Ratdomopurbo, *Ann. Geofis.* **42**, 565 (1999).
6. R. Hennino et al., *Phys. Rev. Lett.* **86**, 3447 (2001); R. Snieder, *Phys. Rev. E* **66**, 046615 (2002).
7. C. Sens-Schönfelder, U. Wegler, *Geophys. Res. Lett.* **33**, L21302 (2006); U. Wegler, C. Sens-Schönfelder, *Geophys. J. Int.* **168**, 1029 (2007).
8. A. Ratdomopurbo, G. Poupinet, *Geophys. Res. Lett.* **22**, 775 (1995); A. Grêt et al., *Geophys. Res. Lett.* **32**, L06304 (2005); G. Poupinet, W. L. Ellsworth, J. Frechet, *J. Geophys. Res.* **89**, 5719 (1984); A. Grêt, R. Snieder, U. Özbay, *Geophys. J. Int.* **167**, 504 (2006).
9. P. M. Roberts, W. S. Phillips, M. C. Fehler, *J. Acoust. Soc. Am.* **91**, 3291 (1992); A. Grêt, R. Snieder, J. Scales, *J. Geophys. Res.* **111**, B03305 (2006); O. I. Lobkis, R. L. Weaver, *Phys. Rev. Lett.* **90**, 254302 (2003).
10. R. Snieder et al., *Annu. Rev. Earth Planet. Sci.* **35**, 653 (2007).
11. R. Snieder, M. Vrijlandt, *J. Geophys. Res.* **110**, B04301 (2005).
12. E. Larose et al., *Phys. Rev. E* **73**, 016609 (2006).
13. M. L. Cowan et al., <http://arxiv.org/abs/cond-mat/0701624>.
14. J. de Rosny et al., *Phys. Rev. Lett.* **90**, 094302 (2003); J. de Rosny, P. Roux, *J. Acoust. Soc. Am.* **109**, 2587 (2001); S. G. Conti et al., *Appl. Phys. Lett.* **84**, 819 (2004).
15. G. Liger-Belair, *Uncorked: The Science of Champagne*, Princeton U. Press, Princeton, NJ (2004).
16. R. L. Weaver, O. I. Lobkis, *Phys. Rev. Lett.* **87**, 134301 (2001); M. Campillo, A. Paul, *Science* **299**, 547 (2003). See also R. L. Weaver, *Science* **307**, 1568 (2005); A. Curtis et al., *Leading Edge* **25**, 1082 (2006); E. Larose et al., *Geophysics* **71**, S111 (2006).
17. R. Snieder, E. Şafak, *Bull. Seismol. Soc. Am.* **96**, 586 (2006); R. Snieder, J. Sheiman, R. Calvert, *Phys. Rev. E* **73**, 066620 (2006).
18. N. M. Shapiro et al., *Science* **307**, 1615 (2005). ■

ScientificWorkPlace®

Mathematical Word Processing • L^AT_EX Typesetting • Computer Algebra

The Gold Standard for Mathematical Publishing

- ◆ Increase productivity
- ◆ Produce stunning documents easily and quickly
- ◆ Typeset documents with L^AT_EX
- ◆ Work with the easiest-to-use computer algebra system

Also available

MuPAD Pro

An integrated and open mathematical problem-solving environment for symbolic and numeric computing

Includes the Beamer Package for slide presentations

To make a parametric animated plot in cylindrical coordinates

1. Type an expression of the form $(r(u, v, t), \theta(u, v, t), z(u, v, t))$
2. With the insertion point in the expression, choose Plot 3D Animated

The next example shows a cone being generated as the line $z = r$ is

The View Orientation is Turn: 20, Tilt: 40.

Plot 3D Animated + Cylindrical

$(-1 + 2r, 2rt, -1 + 2r)$

www.mackichan.com/pt

Visit our website for free trial versions of all our software.
Toll-free: 877-724-9673 • Email: info@mackichan.com

WORLD'S LARGEST INVENTORY OF OPTICAL COMPONENTS

Request your **FREE** copy today!

800.363.1992

www.edmundoptics.com/PT

Edmund

optics | america